

RESEARCH

Open Access



Complement factor H attenuates TNF- α -induced inflammation by upregulating EIF3C in rheumatoid arthritis

Yimeng Jia^{1,2†}, Bin Feng^{3†}, Xin Ji^{4†}, Xinpeng Tian^{1,2}, Lidan Zhao^{1,2}, Jiaxin Zhou^{1,2}, Wen Zhang^{1,2}, Mengtao Li^{1,2}, Yunyun Fei^{1,2,5*}  and Xunyao Wu^{1,2,6*}

Abstract

Objective To explore the role and underlying mechanism of Complement Factor H (CFH) in the peripheral and joint inflammation of RA patients.

Methods The levels of CFH in the serum and synovial fluid were determined by ELISA. The pyroptosis of monocytes was determined by western blotting and flow cytometry. The inflammation cytokine release was tested by ELISA. The cell migration and invasion ability of fibroblast-like synoviocytes (FLS) were tested by Wound healing Assay and transwell assay, respectively. The potential target of CFH was identified by RNA sequencing.

Results CFH levels were significantly elevated in the serum and synovial fluid from RA and associated with high sensitivity C-reactive protein (hs-CRP), erythrocyte sedimentation rate (ESR), and disease activity score 28 (DAS28). TNF- α could inhibit CFH expression, and CFH combined with TNF- α significantly decreased cell death, cleaved-caspase 3, gasdermin E N-terminal (GSDME-N), and inflammatory cytokines release (IL-1 β and IL-6) of RA-derived monocytes. Stimulated with TNF- α increased CFH levels in RA FLS and CFH inhibits the migration, invasion, and TNF- α -induced production of inflammatory mediators, including proinflammatory cytokines (IL-6, IL-8) as well as matrix metalloproteinases (MMPs, MMP1 and MMP3) of RA FLSs. The RNA-seq results showed that CFH treatment induced upregulation of eukaryotic translation initiation factor 3 (EIF3C) in both RA monocytes and FLS. The migration of RA FLSs was promoted and the expressions of IL-6, IL-8, and MMP-3 were enhanced upon EIF3C knockdown under the stimulation of CFH combined with TNF- α .

Conclusion In conclusion, we have unfolded the anti-inflammatory roles of CFH in the peripheral and joints of RA, which might provide a potential therapeutic target for RA patients.

Keywords Complement factor H, Rheumatoid arthritis, Pyroptosis, Fibroblast-like synoviocytes, Eukaryotic translation initiation factor 3 subunit C

[†]Yimeng Jia, Bin Feng and Xin Ji contributed equally to this paper.

*Correspondence:

Yunyun Fei

feiyunyun@pumch.cn

Xunyao Wu

xunyaowu@mail.ustc.edu.cn

Full list of author information is available at the end of the article



© The Author(s) 2023. **Open Access** This article is licensed under a Creative Commons Attribution 4.0 International License, which permits use, sharing, adaptation, distribution and reproduction in any medium or format, as long as you give appropriate credit to the original author(s) and the source, provide a link to the Creative Commons licence, and indicate if changes were made. The images or other third party material in this article are included in the article's Creative Commons licence, unless indicated otherwise in a credit line to the material. If material is not included in the article's Creative Commons licence and your intended use is not permitted by statutory regulation or exceeds the permitted use, you will need to obtain permission directly from the copyright holder. To view a copy of this licence, visit <http://creativecommons.org/licenses/by/4.0/>. The Creative Commons Public Domain Dedication waiver (<http://creativecommons.org/publicdomain/zero/1.0/>) applies to the data made available in this article, unless otherwise stated in a credit line to the data.

Introduction

Rheumatoid arthritis (RA) is a chronic autoimmune disease characterized by progressive synovitis that can lead to severe joint destruction and disability. TNF- α induced inflammation is a critical determinant for RA joint pathogenesis, and targeting TNF- α therapies has achieved significant improvements in RA treatment in recent years. However, a considerable proportion (approximately 40–44%) of patients fail to respond [1].

Recent studies have uncovered the important roles of the complement system in RA. Activated fragments and degradation products of complement are significantly elevated in the joint fluid and peripheral blood of RA patients [2, 3]. Mice deficient for C3aR, C5aR, or C6 led to decreased proximal joint IgG and C3 deposition in comparison to WT mice [4]. C4BP, one of the inhibitors of complement, has been found to have preventive and therapeutic value in collagen-induced arthritis (CIA) [5]. Our previous study has shown that complement C1q could promote monocyte pyroptosis and inflammatory cytokines release plus pentraxin 3 in RA [6].

Complement factor H (CFH) is an abundant soluble complement regulator essential for controlling the alternative pathway in blood and on cell surfaces, which protects cells and tissues from unintended complement-mediated injury [7]. CFH is secreted by cell types, including monocytes, fibroblasts, and endothelial cells, that likely contribute to local titers of the protein in tissues [8]. In collagen antibody induced- arthritis (CAIA) mouse models, complement receptor 2 combined with CFH effectively reduces the severity of joint swelling and cartilage damage [9]. In the present study, we have uncovered the role of CFH in inhibiting TNF- α -induced inflammation in monocytes and fibroblast-like synoviocytes (FLSs) and provided a potential strategy for promoting anti-TNF- α treatment in RA.

Methods

Patients and ethics

All newly-onset RA patients were enrolled in the Peking Union Medical College Hospital, and demographic information was demonstrated in Additional file 2: Table S1. Peripheral blood samples were collected from active RA (11 males and 44 females, aged 49.42 ± 13.25 years) and healthy controls (5 males and 23 females, aged 36.43 ± 11.61 years). Synovial specimens were collected from active RA (2 males and 15 females, aged 57.77 ± 12.4 years) and OA patients (8 males and 6 females, aged 71.26 ± 8.5 years) undergoing knee or hip arthroplasty (Additional file 2: Table S2). RA patients fulfilled the 2010 revised criteria of the ACR-EULAR classification [10].

PBMC isolation and In vitro monocyte purification

Human peripheral blood mononuclear cells (PBMCs) were isolated with Ficoll-Paque density (DAKEWE, China) as previously described. CD14⁺ monocytes were purified using CD14 microbeads (130-107-576, Miltenyi Biotec) and maintained in RPMI 1640 supplemented with 10% fetal bovine serum (FBS) (Gibco, USA), 100 U/ml penicillin and 100 μ g/ml streptomycin (15140122, ThermoFisher).

FLS preparation

The synovial tissue was fully cut into pieces of 2–3 mm² and enzymatically digested with 1 mg/ml type I collagenase (Sigma-Aldrich, St. Louis, MO, USA) in the shaker at 37 °C for 1 h. Following cell dissociation, the samples were filtered through a 70 μ m cell strainer. Fibroblasts were pelleted by centrifugation at 1000 rpm for 10 min and plated in DMEM supplemented with 10% FBS (Gibco; Thermo Fisher Scientific, Waltham, MA, USA) and antibiotics (100 U/ml penicillin, 100 μ g/ml streptomycin; Invitrogen, Carlsbad, CA, USA), and then put in a 37 °C, 5% CO₂ incubator. The medium was changed after the cells adhered to the cell wall for 24 h. Once confluent, FLSs were trypsinized and diluted at a 1:3 split ratio for a new passage. The experiments were restricted to FLSs from passages 3–8.

In vitro stimulation

For cytokines stimulation, freshly isolated monocytes and FLSs were incubated with 50 ng/ml TNF- α (Peprotech, 300-01A), IL-1 β (Peprotech, 200-01B), and IL-6 (Peprotech, 200-06) for 24 h. The dose of CFH (R&D Systems, 4779-FH-050) used in our vitro studies was 5 μ g/ml.

Cell viability assay

Cell viability was determined using a Cell Counting kit-8 (CCK-8 kit, Beyotime, China). 10% Cell Counting Kit-8 (CCK-8) reagent was added to each well and incubated for 30 min. The optical density was measured at 450 nm using a microplate reader (Bio-Rad, United States).

Flow cytometry

Purified monocytes from each RA patient were seeded in 48-well culture plates, after treatment with TNF- α (50 ng/ml) or CFH (5 μ g/ml) for 24 h. The cells were harvested, washed with cold PBS, and stained using an Annexin V-PE/7-AAD Apoptosis Detection Kit (BD PharMingen), according to the manufacturer's

instructions. Cells were then analyzed using a BD FACSAria™ II flow cytometer (BD Biosciences, San Jose, CA, USA).

Wound healing assay

FLSs were seeded in 24-well plates at a density of 1×10^5 cells/well. After the cells had adhered to the wall, they were scratched using pipette tips and then gently washed with PBS. Subsequently, the plate was put under a microscope to take pictures (0 h). After treatment with TNF- α (50 ng/ml) or CFH (5 μ g/ml) in the serum-free medium for 36 h, the scratched areas were photographed at the same magnification at the same position, and the migration area was analyzed.

Transwell assay

FLS invasion was performed using the Boyden chamber method in 24-well plates with 6.5 mm diameter inserts containing 8 μ m pores (Corning, NY, United States). The upper surface of the chambers was coated with Matrigel (50 μ g/Well, BD Biosciences, Oxford, United Kingdom) which mimics the extracellular matrix. The FLSs (5×10^4 cells in 200 μ l) were suspended in a serum-deprived medium containing TNF- α (50 ng/ml), CFH (5 μ g/ml), TNF- α +CFH (50 ng/ml and 5 μ g/ml, respectively), and plated in the upper chamber. Simultaneously, a culture medium containing 10% FBS (600 μ l) was placed in the lower chamber as a chemoattractant. Afterward, the system was incubated for 36 hours. Then FLSs were fixed with paraformaldehyde for 30 min and stained with 0.1% crystal violet for 20 min. The cells on the top surface of the membrane were scraped using a cotton swab, and then FLSs that migrated to the lower side were photographed under the microscope at 200 magnification. Five fields were randomly selected for cell counting using the ImageJ software, and the mean number of stained FLSs was calculated.

Quantitative real-time PCR

After different treatments, total RNA was isolated from RA-FLS cells using TRIzol reagent (Invitrogen, USA). Then, total RNA was further reverse-transcribed into cDNA using the Prime Script RT Reagent Kit (Takara, China). The primers used for real-time PCR are listed in Additional file 2: Table S3. On the ABI-7500 Thermal Cycler (Applied Biosystems, USA), we used SYBR Green quantitative real-time polymerase chain reaction (qRT-PCR) (Takara, China) analysis to detect mRNA levels of every gene. Results were shown in the form of relative expression calculated by the $2^{-\Delta\Delta CT}$ method.

Enzyme-linked immunosorbent assay (ELISA)

Levels of CFH, IL-1 β , IL-6, IL-8, MMP-1, and MMP-3 in the cell culture supernatant were measured with commercially available standard sandwich enzyme-linked kits.

Western blotting

Proteins were separated by 10% SDS-PAGE and then transferred to a polyvinylidene fluoride (PVDF) membrane (Millipore, USA). The membranes were blocked with QuickBlock™ Blocking Buffer followed by incubation with primary antibodies, including anti-cleaved caspase 3 (9664S, Cell Signaling Technology), anti-GSDME (NBP2-80426, Novus Biological) and anti-EIF3C (NB100-511, Novus Biologicals), anti- β -actin (ab32503, Abcam) overnight at 4 °C. The membranes were washed three times and incubated with secondary anti-rabbit IgG (#7074, Cell Signaling Technology) or anti-mouse IgG (#7076, Cell Signaling Technology) for 1 h. Protein bands were visualized on the Western blotting detection system (Bio-Rad, USA)

siRNAs transfection

Small interfering RNA (siRNA) against EIF3C and negative control siRNAs were synthesized by RiboBio (Guangzhou, China). The siRNA sequences are shown in Additional file 2: Table S3. Cells were cultured at 70–80% confluence and transfected with siRNAs using Lipofectamine 3000 reagent (Thermo Fisher Scientific, United States) following the manufacturer's protocol.

RNA sequencing and data analysis

For RNA sequencing, total RNA was extracted by the TRIzol method and quantified using a NanoDrop ND-1000 instrument. cDNA library construction for RNA transcriptome sequencing was performed by Beijing Novogene (Beijing, China), and volcano plots were performed for the differentially expressed genes (DEGs) using R 3.6.3 edge R software for statistical computing and graphics.

Statistical analysis

Data are presented as mean \pm standard error of measurement (SEM). The data were first performed with the normality distribution. Statistical analysis was performed using GraphPad Prism 8.0.1 software with one-way ANOVA. Two group comparisons were completed using a 2-tailed Student's t-test or the Mann-Whitney test. The Pearson correlation analysis was adopted.

The value of $P < 0.05$ was considered to be statistically significant.

Results

CFH is elevated in the serum and synovial fluid and correlated with disease activity in RA

We first carried out ELISA to determine CFH levels in RA patients (Fig. 1A, B). We found that CFH was significantly higher in serum or synovial fluid of RA patients compared with those of healthy controls ($606.6 \pm 185.8 \mu\text{g/ml}$ vs $472.4 \pm 96.7 \mu\text{g/ml}$, $p=0.0003$) or osteoarthritis patients ($126.8 \pm 29.2 \mu\text{g/ml}$ vs $46.5 \pm 16.3 \mu\text{g/ml}$, $p=0.0005$). In addition, correlation analysis showed that CFH levels were positively correlated with ESR ($r = 0.55$, $P < 0.0001$), DAS28 ($r = 0.56$, $P < 0.0001$), and hs-CRP ($r=0.56$, $P < 0.0001$, Fig. 1C).

CFH attenuates TNF- α -induced pyroptosis and inflammatory cytokines release of RA monocytes

We isolated monocytes and stimulated them with RA-related cytokines in vitro, including TNF- α , IL-1 β , and IL-6, IL-18, IL-17A, GM-CSF, and IL-10 for 24 hours and detected CFH expression. TNF- α could increase CFH levels in HC-derived monocytes but inhibit CFH expression in RA-derived monocytes (Fig. 2A and Additional file 2: Fig. S1A). Pro-inflammatory cytokines such as TNF, IL-6, and IL-1, are abundant in the synovium and synovial fluid in RA [11]. According to a 2019 scRNA-seq study, IL-6 is produced mainly by synovial fibroblasts, and macrophages are the main producers of IL-1 and TNF [12]. We therefore investigate the role of CFH in TNF- α -induced inflammation of RA-derived monocytes. As shown in Fig. 2B, CFH could significantly inhibit TNF- α -induced IL-1 β and IL-6 release in RA-derived monocytes, indicating that CFH has an anti-inflammatory effect on RA.

A previous study has reported that TNF- α could induce pyroptosis in RA-derived monocytes by activating the

caspace 3/GSDME pathway [13]. We therefore further investigated the effects of CFH on TNF- α -induced pyroptosis in RA-derived monocytes. Using flow cytometry, CFH+TNF- α decreased the percentage of 7-AAD-positive cells induced by TNF- α (Fig. 2C). Moreover, CFH combined with TNF- α significantly decreased c-Casp-3. TNF- α increased the expression of c-Casp-3, although there was no significant difference. TNF- α significantly increased the expression of GSDME-N, while CFH could inhibit TNF-induced GSDME-N expression. The expression of GSDME-F was not significantly different between groups (Fig. 2D). The typical morphologic changes characterized by cell swelling and large bubble blowing were also observed in each group (Fig. 2E). Taken together, these results indicate that CFH attenuates TNF- α -induced pyroptosis in peripheral blood monocytes from RA patients.

CFH inhibits the migration, invasion, and TNF- α -induced expression of inflammatory mediators of RA FLSs

We further investigate the effect of CFH on local inflammation in RA patients. We found that stimulation with TNF- α could increase the mRNA and protein levels of CFH both in RA and OA FLS (Fig. 3A and Additional file 2: Fig. S1B). Moreover, we found that CFH could significantly inhibit the migration and invasion ability of RA-FLS and OA-FLS (Fig. 3B–E). The cell-to-cell contact between RA fibroblasts and macrophages in the lining layer provokes IL-6 and IL-8 production and amplifies the inflammatory signaling cascades [14]. In accordance with what we observed in monocytes, CFH could also suppress TNF- α -induced proinflammatory cytokines (IL-6, IL-8). RA-FLS also secrete a variety of matrix metalloproteinases (MMPs) to drive joint destruction, among these, MMP-1 and MMP-3 can directly destroy type II collagen and thus promote cartilage destruction [15]. In particular, MMP-3 is a reliable marker of rheumatoid arthritis disease activity, imaging monitoring, prognosis,

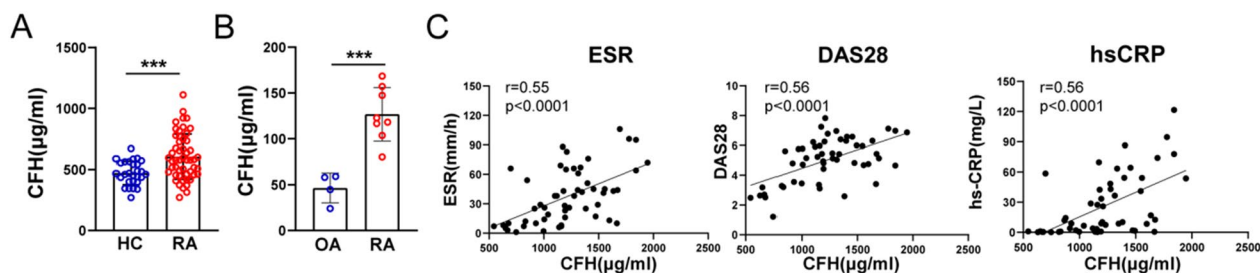


Fig. 1 CFH is elevated in the serum and synovial fluid from RA. **A** CFH in serum from RA patients and healthy control detected by ELISA. (RA: $n=52$; HC: $n=28$). **B** CFH in synovial fluid from RA and OA patients detected by ELISA. (RA: $n=8$; OA: $n=4$). **C** Correlation analysis of CFH expression in serum of RA patients with ESR, DAS28, and hs-CRP respectively. Data are expressed as mean \pm SEM. *** $p < 0.001$; RA: rheumatoid arthritis; OA: osteoarthritis; HC: healthy control; hs-CRP: high sensitivity C-reactive protein; ESR: erythrocyte sedimentation rate; DAS28: disease activity score 28

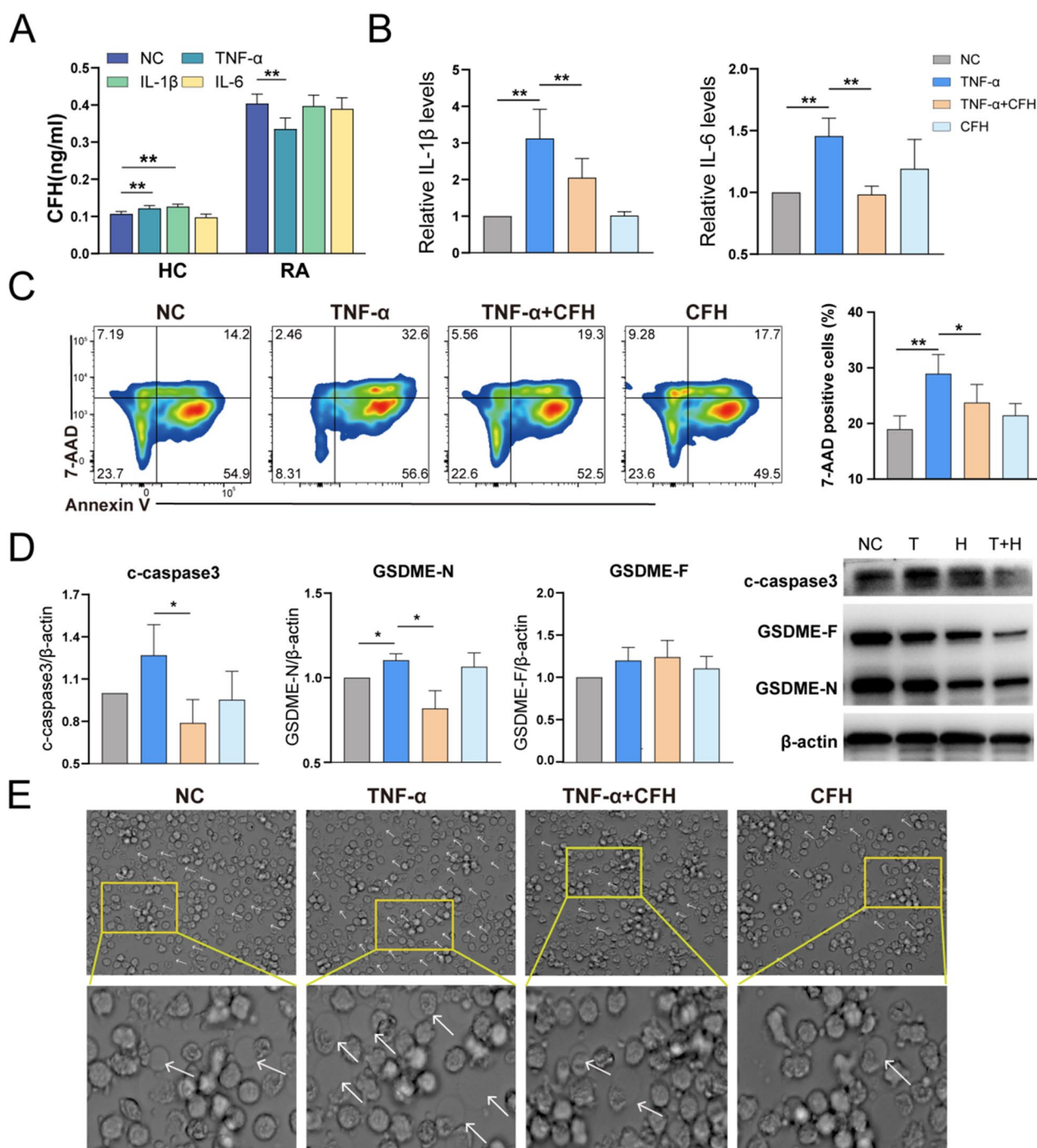


Fig. 2 CFH attenuates TNF-α-induced pyroptosis and inflammatory cytokines release of RA monocytes. Purified CD14⁺ monocytes were pretreated with TNF-α(50 ng/ml), TNF-α(50 ng/ml) + CFH (5 μg/ml), or CFH (5 μg/ml) for 24 h (n = 6–9). **A** The expression of secreted CFH in the culture supernatant of RA patients and healthy control stimulated with TNF-α, IL-1β, and IL-6 detected by ELISA. **B** The expression of secreted cytokines (IL-1β, IL-6) in the culture supernatant of RA monocytes in each group was detected by ELISA. **C** Flow cytometric analysis of cells stained with annexin V/7-AAD to determine cell death and percentage of 7-AAD-positive cells. **D** The protein expression of c-caspase3, GSDME-N, and GSDME-F was measured by using Western blot. **E** Representative phase-contrast microscopy images of monocytes treated as indicated. Arrows indicate pyroptotic cell bubbles. Data are expressed as mean ± SEM. *p < 0.05; **p < 0.01; NC: negative control; T: TNF-α; T + H: TNF-α + CFH; H: CFH; IL-6: interleukin-6; IL-1β: interleukin-1β; c-caspase3: cleaved caspase-3; GSDME-N: gasdermin E N-terminal; GSDME-F: gasdermin E full length

and response to treatment [16]. CFH could suppress TNF- α -induced production of MMP1 and MMP3 in the RA-FLS cells (Fig. 3F, G). However, CFH did not affect cell viability in both RA-FLS and OA-FLS (Additional file 2: Fig. S2) and exhibited only a mild effect on TNF- α induced inflammatory factors in OA-FLS (Fig. 3E, G). Taken together, these results support a protective role of CFH in RA, which could both inhibit the migration and invasion of FLS and attenuate TNF-induced inflammation in RA FLS and monocytes.

EIF3C is a potential target for CFH to play a role in inhibiting FLS function

To gain insights into the molecular mechanism of CFH, we performed RNA sequencing of CFH-treated and untreated FLSs from three RA patients. A total of 105 upregulated genes and 76 downregulated genes (with P value <0.05 and $|\log_2FC| >0.5$) were detected and visualized by volcano plot (Fig. 4A). CFH-treated and untreated monocytes were also used to carry out RNA sequencing from four RA patients. The volcano plot showed a total of 246 upregulated genes and 218 downregulated genes (with P value <0.05 and $|\log_2FC| >0.5$) (Fig. 4B). A detailed list of the differentially expressed genes is shown in Additional file 1. To identify the genes that play an important role in both RA-derived monocytes and FLSs, the upregulated genes related to the CFH treatment in monocytes and FLS were selected, and the intersecting proteins were identified. One gene was obtained, namely, EIF3C (eukaryotic translation initiation factor 3 subunit C) (Fig. 4C). We found both EIF3C and EIF3CL (eukaryotic translation initiation factor 3 subunit C like) were upregulated in the CFH-treated monocytes (Fig. 4D). The genetic sequence and encoded protein of EIF3CL are nearly identical to that of EIF3C. Moreover, EIF3C is the top 1 upregulated differentially expressed gene according to the P value in the CFH-treated FLS (Fig. 4A). Thus, we focused on EIF3C.

We used Western blotting to verify the reliability of RNA-seq. The results showed a significant increase in the EIF3C protein level in CFH-treated monocytes compared to the negative control (Fig. 4E). To further investigate

whether the anti-inflammatory effect of CFH on TNF- α is also dependent on EIF3C, we assessed the effect of TNF- α and CFH on EIF3C expression in monocytes and FLS, respectively. The results are shown in Fig. 4F. The expression of EIF3C was significantly increased in both RA-derived monocytes and FLS with CFH and TNF- α combined stimulation.

EIF3C knockdown upregulated TNF- α -induced expression of proinflammatory cytokines and MMPs

Finally, we used siRNA oligonucleotide sequences to downregulate the expression of EIF3C and further investigate the role of EIF3C in regulating RA FLS function. Both RT-qPCR and WB results showed that EIF3C-siRNA decreased the expression of CFH (Additional file 2: Fig. S3). As shown in Fig. 5A, the migration of RA FLSs was promoted upon EIF3C knockdown under the stimulation of CFH combined with TNF- α . However, there were no significant changes in the invasion of RA FLSs (Fig. 5B). In addition, we found that EIF3C knockdown also upregulated the expression of IL-6, IL-8, and MMP-3 (Fig. 5C). These data suggested that EIF3C is a potential target for CFH to play a role in inhibiting FLS function induced by TNF- α .

Discussion

In this study, we have unfolded the anti-inflammatory roles of CFH in RA. We showed that CFH could inhibit the migration and invasion of FLS. Moreover, we found that CFH could dampen the inflammatory status of RA by inhibiting TNF- α -induced monocytes pyroptosis as well as inflammatory mediator production of monocytes and FLSs.

RA-FLS migration and invasion are pivotal contributors to synovitis and bone destruction. Many studies have shown that RA-FLS maintain their invasive, tumor-like phenotype despite previous passaging in vitro [17, 18]. A recent study demonstrated that synovial fibroblasts exhibited enhanced metabolic activity inducing functional changes with intensified migration, invasiveness, and osteoclastogenesis after repeated inflammatory challenges, which depended on intracellular complement C3

(See figure on next page.)

Fig. 3 CFH inhibits the migration, invasion, and TNF- α -induced expression of inflammatory mediators of RA FLSs. The FLSs were pretreated with TNF- α (50 ng/ml), TNF- α (50 ng/ml) + CFH (5 μ g/ml), or CFH (5 μ g/ml) for 24 h (n = 5–10). **A** The expression of secreted CFH in the culture supernatant of RA-FLS and OA-FLS detected by ELISA. **B–C** The effect of CFH on cell migration was detected using wound healing assay. The scratching area was photographed at 0 h and 24 h. The scratch assay was presented as the percentage by which the original scratch area decreased at 24 h. Representative images (original magnification, $\times 200$) are shown. **D–E** FLS invasion ability was measured by Transwell assay, and the invaded cells were photographed. The relative invasion rate was calculated by counting mean invaded cells from 5 randomly selected fields and then normalized to that in the NC group. Representative images (original magnification, $\times 200$) are shown. **F–G** The expression of secreted cytokines (IL-6, IL-8) and MMPs (MMP-1, MMP-3) in culture supernatant of RA-FLS and OA-FLS in each group were detected by ELISA. Data are expressed as mean \pm SEM. *p < 0.05; **p < 0.01; ***p < 0.001; ****p < 0.0001. MMP-1: matrix metalloproteinase-1; MMP-3: matrix metalloproteinase-3

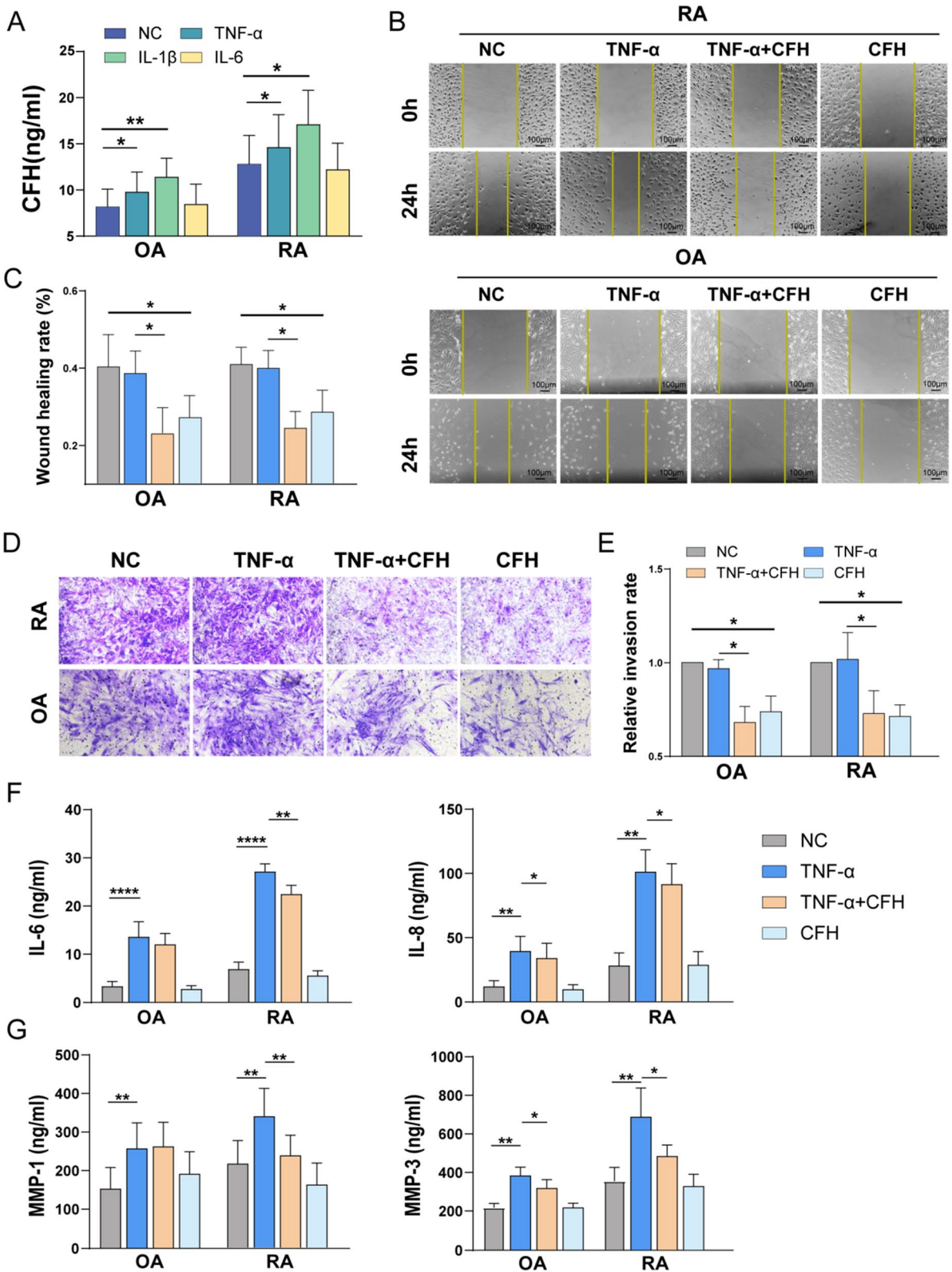


Fig. 3 (See legend on previous page.)

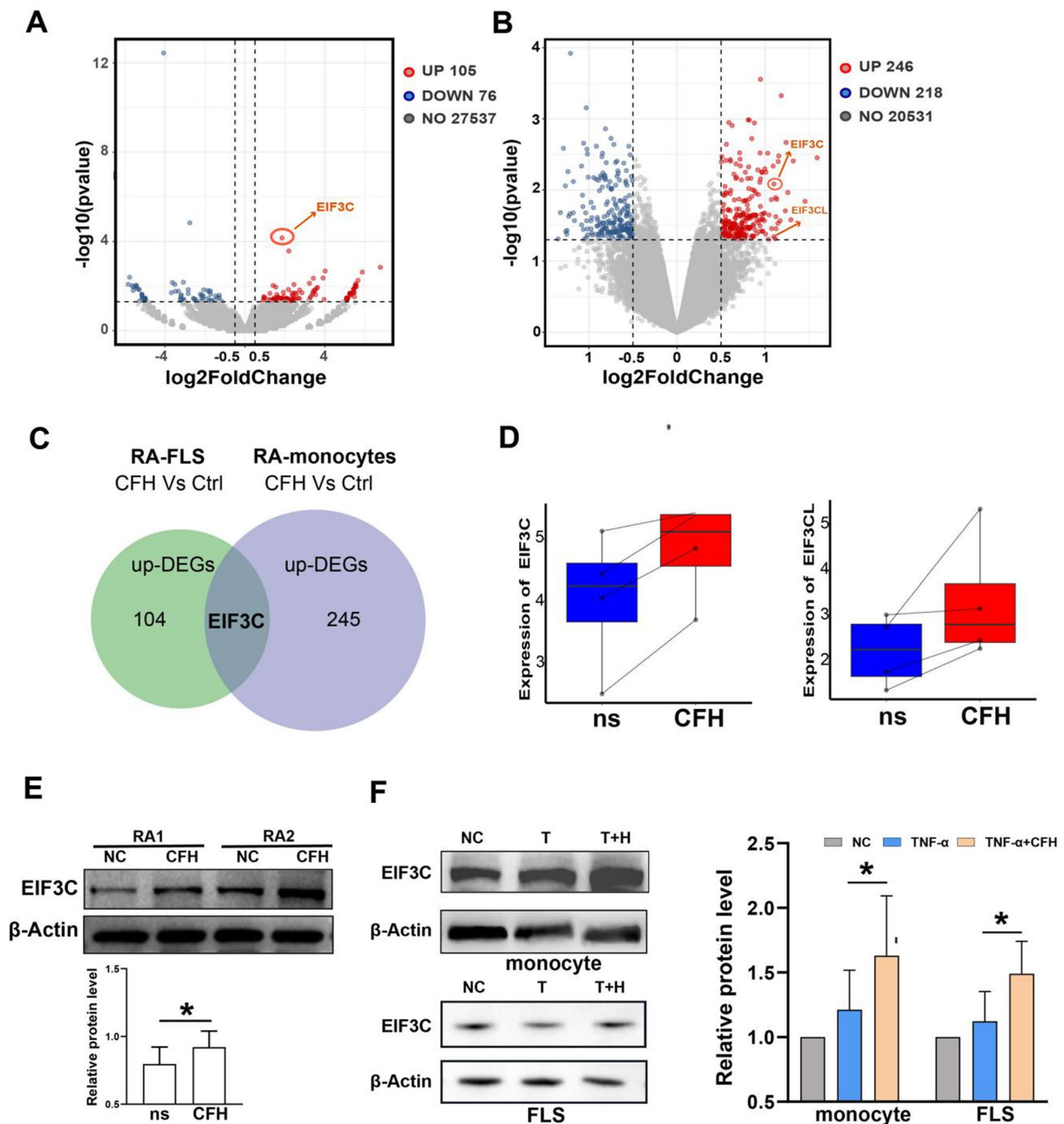


Fig. 4 EIF3C is a potential target for CFH to play a role in inhibiting FLSs and monocyte function. Monocytes and FLS from RA patients were selected respectively, and cells from each patient were divided into two groups. One group was left untreated, and one group was treated with 5 $\mu\text{g/ml}$ CFH for 6 h. **A** Volcano plot indicated up-regulated (red dots) and down-regulated (blue dots) genes (P value < 0.05 and $|\log_2\text{FC}| > 0.5$) by RNA sequencing in CFH-treated versus untreated RA monocytes. EIF3C is indicated. **B** Volcano plot indicated up-regulated (red dots) and down-regulated (blue dots) genes (P value < 0.05 and $|\log_2\text{FC}| > 0.5$) by RNA sequencing in CFH-treated versus untreated RA monocytes. EIF3C and EIF3CL are indicated. **C** We selected the genes upregulated in the CFH-treated monocytes and the genes upregulated in the CFH-treated FLS identified by RNA-sequencing and determined the intersecting proteins. We obtained one gene, namely EIF3C. DEGs: Differentially Expressed Genes. **D** The boxplot shows the relative expression of EIF3C and EIF3CL. **E** CFH upregulated the protein expression of EIF3C by using Western blot. **F** CFH combined with TNF- α upregulated protein expression of EIF3C in both RA FLSs and monocytes by using Western blot. Data are expressed as mean \pm SEM ($n = 6$). * $p < 0.05$

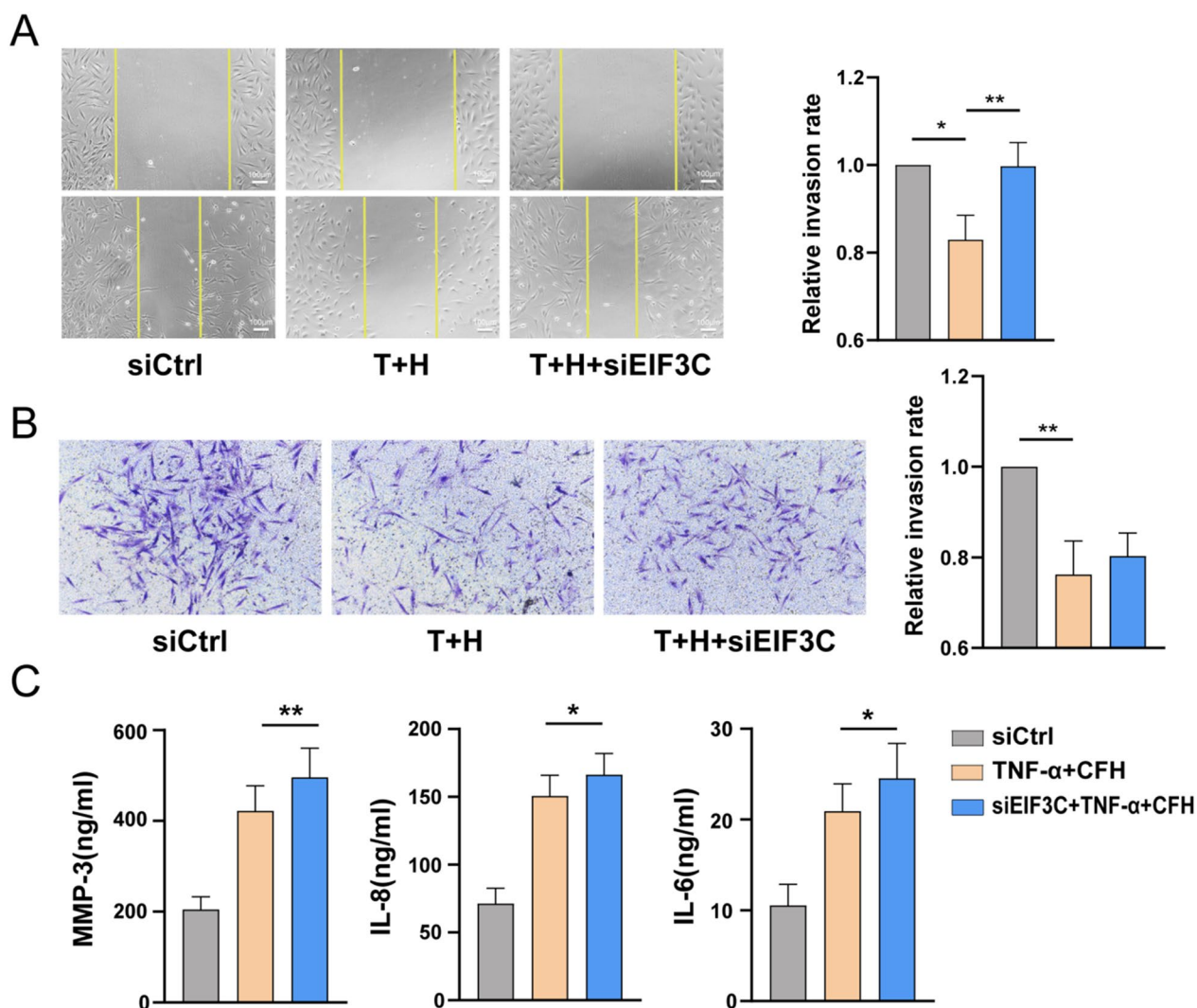


Fig. 5 Effect of CFH knockdown on the function of RA FLS. RA FLSs were transfected with siRNAs for EIF3C (siEIF3C) or control siRNA (siCtrl) for 72 h and then stimulated with TNF-α(50 ng/ml) + CFH (5 μg/ml) for 24 h (n = 4–8). **A** Effect of EIF3C knockdown on the migration of RA FLSs was measured with the wound-healing assay. The relative migration rates were calculated by the percentage by which the original scratch area decreased and then normalized to that in the control group. **B** Effect of EIF3C knockdown on the invasion of RA FLSs using Transwell assay. The relative invasion rates were calculated by counting invaded cells and then normalized to that in the control group. Representative images (original magnification, × 200) are shown. **C** Effect of EIF3C knockdown on the inflammatory mediators of RA FLSs detected by ELISA. Data show the mean ± SEM. *p < 0.05; **p < 0.01

and C3a receptor expression [19]. CFH could accelerate the decay of the alternative pathway C3 convertase (C3b, Bb) [8]. Here, we found that CFH could directly inhibit RA-FLS migration and invasion. It would be an interesting topic to further explore the underline molecular mechanism and potential therapeutic targets to revert the phenotype of RA-FLS.

Our previous study has uncovered the role of complement C1q with its ligand PTX3 in promoting NLRP3 inflammasome over-activation, GSDMD-conferred pyroptosis, and inflammatory cytokine release in

RA-derived monocytes [6]. A recent study by Zhai et al. supports the notion of a pathogenic role of GSDME [13]. Here, we have found that TNF-α could induce increased expression of GSDME-N, while CFH, in combination with TNF-α, significantly decreased the expression of cleaved caspase-3 and GSDME-N. Moreover, TNF-α could suppress CFH production in RA-derived monocytes, while this observation is the opposite in HC-derived monocytes. These suggest TNF-α exacerbates pyroptosis-conferred inflammation by inhibiting CFH production in RA patients. However, whether there is

any interaction between the complement system and TNF- α is still a controversial issue [20]. TNF- α seems to activate the complement system, as demonstrated by a reduction of complement cleavage products in sera of patients treated with anti-TNF agents [21]. A mechanism proposed is that anti-TNF α decreases plasma levels of CRP, which can activate complement cascade through the classical pathway [22].

Our study also found that CFH significantly inhibited the secretion of TNF-induced inflammatory factors of local FLS in joints through upregulating EIF3C. EIF3C, one of the 13 subunits of eIF3 factor, is highly conserved in evolution and constitutes the function core of eIF3 with the other five subunits. EIF3C plays a very important role during development and homeostasis. Research on eIF3 is mostly concentrated in malignant tumors. EIF3C promotes the proliferation, migration, and invasion of prostate cancer, pancreatic cancer, and lung adenocarcinoma [23–25]. It has also been found that expression of EIF3C in HCC cells reduced transwell cell migration [26]. However, knockdown EIF3C did not revert CFH-induced RA-FLS invasion significantly, indicating that the role of CFH was not dependent on EIF3C. Interestingly, the knockdown of EIF3C reversed the anti-inflammatory role of CFH in TNF- α -induced FLS inflammation. Recent studies suggest that the knockdown of EIF3C can increase the expression of caspase 3 to promote apoptosis [27]. Caspase 3 could convert TNF- α -induced apoptosis to cell pyroptosis and lead to inflammatory injury [28]. Therefore, it is hypothesized that CFH protects against the TNF-induced Casp-3-GSDME pyroptosis pathway by increasing the expression of EIF3C. Further studies are required to identify the related signaling pathways of CFH on RA and determine its relief effect on RA in vivo.

In this study, TNF- α did not promote FLS migration and invasion, which is also found in another study [29]. RA animal models demonstrated that TNF is not able on its own to promote synovial invasion and attachment to cartilage and bone. The study of hTNF transgenic mice showed that these processes were dependent on the presence of IL-1 or cartilage damage [30, 31].

IL-1 is a master cytokine of local and systemic inflammation. In patients failing TNF α blockers, IL-1 blockade is effective in controlling disease activity [32]. We found that IL-1 β could significantly promote the expression of CFH in FLSs and healthy controls-derived monocytes. IL-1/IL-1R signaling induced by all-trans-retinal contributes to complement alternative pathway activation in retinal pigment epithelium [33]. Interaction of factor H with its receptor could stimulate the secretion of IL-1 β by monocytes [34]. A

miR-146a–CFH–IL-1 β loop circuit was found to initiate a cascade of inflammation in temporal lobe epilepsy [35]. Therefore, we would further our research on whether CFH can also inhibit IL-1 β -induced inflammation in RA patients.

In summary, this study shows that CFH levels may reflect the presence of an underlying inflammatory process in RA and plays a negative feedback-regulating role under TNF stimulation. CFH plays an important protective role in the joint via suppressing the migration and invasion of RA-FLS. Furthermore, CFH attenuates TNF- α -induced inflammation by upregulating EIF3C. Possible intervention strategies could be explored further to target CFH-related signaling pathways in anti-TNF-resistant RA patients.

Supplementary Information

The online version contains supplementary material available at <https://doi.org/10.1186/s12967-023-04730-2>.

Additional file 1: A detailed list of the differentially expressed genes of RA-derived monocytes and FLS.

Additional file 2: Figure S1. A Monocytes were treated with IL-18, IL-17A, GM-CSF, and IL-10 (50 ng/ml) for 24 h. The expression of secreted CFH in the culture supernatant of RA patients was detected by ELISA. **B** FLS were treated with TNF- α , IL-1 β , and IL-6 (50 ng/ml) for 24 h. The expression of CFH in RA-FLS and OA-FLS stimulated with TNF- α , IL-1 β , and IL-6 was detected by qPCR. Data are expressed as mean \pm SEM (n=6-8). *p < 0.05.

Figure S2. Cells were treated with TNF- α (50ng/ml) or TNF- α (50 ng/ml) +CFH (5 μ g/ml) or CFH (5 μ g/ml) for 24 h. The CCK-8 assay was used to detect cell viability. Data are expressed as mean \pm SEM (n=6).

Figure S3. The efficiency of EIF3C knockdown was detected by RT-qPCR analysis and Western blotting. Data are expressed as mean \pm SEM (n=5). **p < 0.01; ***p < 0.001. **Table S1.** Demographic and clinical features of included RA patients. **Table S2.** Demographic and clinical features of patients with OA. **Table S3.** Sequences of primers for RT-qPCR and siRNA oligonucleotides

Acknowledgements

We thank all the members of the National Clinical Research Center for Dermatologic and Immunologic Diseases (NCRC-DID) for helpful discussion and support.

Author contributions

YMJ, BF, and XJ were responsible for methodology, formal analysis, and original draft; XPT, LDZ, and JXZ provided methodology and resources; MTL and WZ were involved in project administration and supervision; XYW and YYF took part in conceptualization, funding acquisition, and finalization of the manuscript. All authors revised the paper critically for important intellectual content and gave their final approval for submission.

Funding

This work was supported by the National Natural Science Foundation of China (81971544, 81971545), the Chinese National Key Technology R&D Program, Ministry of Science and Technology (2022YFC2504600), and the National High Level Hospital Clinical Research Funding (2022-PUMCH-B -013).

Availability of data and materials

Data from RNA sequencing have been deposited in National Genomics Data Center (NGDC) and are accessible through the GSA-human Series accession number [HRA005914]. The rest of the data generated during this study is available within the article or its supplementary materials.

Declarations

Ethics approval and consent to participate

The study was approved by the Ethics Committee of the Peking Union Medical College Hospital (No: JS-2905) and was conducted following the Helsinki Declaration. Informed consent of all the patients was obtained.

Consent for publication

The manuscript is approved by all authors for publication.

Competing interests

The authors have declared no competing interests.

Author details

¹Department of Rheumatology and Clinical Immunology, Chinese Academy of Medical Sciences, Peking Union Medical College Hospital, Peking Union Medical College, Beijing, China. ²The Ministry of Education Key Laboratory, National Clinical Research Center for Dermatologic and Immunologic Diseases (NCRC-DID), Beijing, China. ³Department of Orthopedic Surgery, Peking Union Medical College Hospital, Chinese Academy of Medical Science and Peking Union Medical College, Beijing 100730, China. ⁴Department of Nuclear Medicine, The First Affiliated Hospital of Nanjing Medical University, Jiangsu Province Hospital, Nanjing, China. ⁵Department of Health and Medicine, Peking Union Medical College Hospital, Chinese Academy of Medical Sciences, Peking Union Medical College, Beijing, China. ⁶Department of Medical Research Center, Peking Union Medical College Hospital, Chinese Academy of Medical Science and Peking Union Medical College, Beijing, China.

Received: 5 September 2023 Accepted: 12 November 2023

Published online: 23 November 2023

References

- Conigliaro P, Triggianese P, De Martino E, Fonti GL, Chimenti MS, Sunzini F, et al. Challenges in the treatment of rheumatoid arthritis. *Autoimmun Rev*. 2019;18(7):706–13.
- Aggarwal A, Bhardwaj A, Alam S, Misra R. Evidence for activation of the alternate complement pathway in patients with juvenile rheumatoid arthritis. *Rheumatology*. 2000;39(2):189–92.
- Wouters D, Voskuyl AE, Molenaar ETH, Dijkmans BAC, Hack CE. Evaluation of classical complement pathway activation in rheumatoid arthritis: measurement of C1q–C4 complexes as novel activation products. *Arthritis Rheum*. 2006;54(4):1143–50.
- Banda NK, Hyatt S, Antonielli AH, White JT, Glogowska M, Takahashi K, et al. Role of C3a receptors, C5a receptors, and complement protein C6 deficiency in collagen antibody-induced arthritis in mice. *J Immunol*. 2012;188(3):1469–78.
- Blom AM, Nandakumar KS, Holmdahl R. C4b-binding protein (C4BP) inhibits development of experimental arthritis in mice. *Ann Rheum Dis*. 2009;68(1):136–42.
- Wu X-Y, Li K-T, Yang H-X, Yang B, Lu X, Zhao L-D, et al. Complement C1q synergizes with PTX3 in promoting NLRP3 inflammasome over-activation and pyroptosis in rheumatoid arthritis. *J Autoimmun*. 2020;106:102336.
- Ferluga J, Kouser L, Murugaiah V, Sim RB, Kishore U. Potential influences of complement factor H in autoimmune inflammatory and thrombotic disorders. *Mol Immunol*. 2017;84:84–106.
- Ferreira VP, Pangburn MK, Cortés C. Complement control protein factor H: the good, the bad, and the inadequate. *Mol Immunol*. 2010;47(13):2187–97.
- Banda NK, Levitt B, Glogowska MJ, Thurman JM, Takahashi K, Stah GL, et al. Targeted inhibition of the complement alternative pathway with complement receptor 2 and factor H attenuates collagen antibody-induced arthritis in mice. *J Immunol*. 2009;183(9):5928–37.
- Kay J, Upchurch KS. ACR/EULAR 2010 rheumatoid arthritis classification criteria. *Rheumatology*. 2012;51(Suppl 6):5–9.
- Komatsu N, Takayanagi H. Mechanisms of joint destruction in rheumatoid arthritis—immune cell-fibroblast-bone interactions. *Nat Rev Rheumatol*. 2022;18(7):415–29.
- Zhang F, Wei K, Slowikowski K, Fonseka CY, Rao DA, Kelly S, et al. Defining inflammatory cell states in rheumatoid arthritis joint synovial tissues by integrating single-cell transcriptomics and mass cytometry. *Nat Immunol*. 2019;20(7):928–42.
- Zhai Z, Yang F, Xu W, Han J, Luo G, Li Y, et al. Attenuation of rheumatoid arthritis through the inhibition of tumor necrosis factor-induced caspase 3/gasdermin e-mediated pyroptosis. *Arthritis Rheumatol*. 2022;74(3):427–40.
- Elshabrawy HA, Chen Z, Volin MV, Ravella S, Virupannavar S, Shahrara S. The pathogenic role of angiogenesis in rheumatoid arthritis. *Angiogenesis*. 2015;18(4):433–48.
- Grillet B, Pereira RVS, Van Damme J, Abu El-Asrar A, Proost P, Opendakker G. Matrix metalloproteinases in arthritis: towards precision medicine. *Nat Rev Rheumatol*. 2023;19(6):363–77.
- Lerner A, Neidhöfer S, Reuter S, Matthias T. MMP3 is a reliable marker for disease activity, radiological monitoring, disease outcome predictability, and therapeutic response in rheumatoid arthritis. *Best Pract Res Clin Rheumatol*. 2018;32(4):550–62.
- Sfikakis PP, Vlachogiannis NI, Christopoulos PF. Cadherin-11 as a therapeutic target in chronic, inflammatory rheumatic diseases. *Clin Immunol*. 2017;176:107–13.
- Korb-Pap A, Bertrand J, Sherwood J, Pap T. Stable activation of fibroblasts in rheumatic arthritis-causes and consequences. *Rheumatology*. 2016;55(suppl 2):ii64–7.
- Friščić J, Böttcher M, Reinwald C, Bruns H, Wirth B, Popp S-J, et al. The complement system drives local inflammatory tissue priming by metabolic reprogramming of synovial fibroblasts. *Immunity*. 2021;54(5):1002–1021.e10.
- Ballanti E, Perricone C, di Muzio G, Kroegler B, Chimenti MS, Graceffa D, et al. Role of the complement system in rheumatoid arthritis and psoriatic arthritis: relationship with anti-TNF inhibitors. *Autoimmun Rev*. 2011;10(10):617–23.
- Mitoma H, Horiuchi T, Tsukamoto H, Tamimoto Y, Kimoto Y, Uchino A, et al. Mechanisms for cytotoxic effects of anti-tumor necrosis factor agents on transmembrane tumor necrosis factor alpha-expressing cells: comparison among infliximab, etanercept, and adalimumab. *Arthritis Rheum*. 2008;58(5):1248–57.
- Familian A, Voskuyl AE, van Mierlo GJ, Heijst HA, Twisk JWR, Dijkmans BAC, et al. Infliximab treatment reduces complement activation in patients with rheumatoid arthritis. *Ann Rheum Dis*. 2005;64(7):1003–8.
- Liu H, Qin Y, Zhou N, Ma D, Wang Y. ZNF280A promotes lung adenocarcinoma development by regulating the expression of EIF3C. *Cell Death Dis*. 2021;12(1):39.
- Jiao H, Zeng L, Yang S, Zhang J, Lou W. Knockdown EIF3C suppresses cell proliferation and increases apoptosis in pancreatic cancer cell. *Dose Response*. 2020;18(3):1559325820950061.
- Hu J, Luo H, Xu Y, Luo G, Xu S, Zhu J, et al. The prognostic significance of EIF3C gene during the tumorigenesis of prostate cancer. *Cancer Invest*. 2019;37(4–5):199–208.
- Lee H-Y, Chen C-K, Ho C-M, Lee S-S, Chang C-Y, Chen K-J, et al. EIF3C-enhanced exosome secretion promotes angiogenesis and tumorigenesis of human hepatocellular carcinoma. *Oncotarget*. 2018;9(17):13193–205.
- Zhao W, Li X, Wang J, Wang C, Jia Y, Yuan S, et al. Decreasing eukaryotic initiation factor 3C (EIF3C) suppresses proliferation and stimulates apoptosis in breast cancer cell lines through mammalian target of rapamycin (mTOR) pathway. *Med Sci Monit*. 2017;23:4182–91.
- Wang Y, Gao W, Shi X, Ding J, Liu W, He H, et al. Chemotherapy drugs induce pyroptosis through caspase-3 cleavage of a gasdermin. *Nature*. 2017;547(7661):99–103.
- Mosquera N, Rodriguez-Trillo A, Blanco FJ, Mera-Varela A, Gonzalez A, Conde C. All-trans retinoic acid inhibits migration and invasiveness of rheumatoid fibroblast-like synoviocytes. *J Pharmacol Exp Ther*. 2020;372(2):185–92.
- Hillen J, Geyer C, Heitzmann M, Beckmann D, Krause A, Winkler I, et al. Structural cartilage damage attracts circulating rheumatoid arthritis synovial fibroblasts into affected joints. *Arthritis Res Ther*. 2017;19(1):40.
- Korb-Pap A, Stratis A, Mühlberg K, Niederreiter B, Hayer S, Echtermeyer F, et al. Early structural changes in cartilage and bone are required for the attachment and invasion of inflamed synovial tissue during destructive inflammatory arthritis. *Ann Rheum Dis*. 2012;71(6):1004–11.

32. Gabay C, Lamacchia C, Palmer G. IL-1 pathways in inflammation and human diseases. *Nat Rev Rheumatol*. 2010;6(4):232–41.
33. Cheng X, He D, Liao C, Lin S, Tang L, Wang Y-L, et al. IL-1/IL-1R signaling induced by all-trans-retinal contributes to complement alternative pathway activation in retinal pigment epithelium. *J Cell Physiol*. 2021;236(5):3660–74.
34. Ifferoudjane D, Schouft MT, Lemercier C, Gilbert D, Fontaine M. Evidence for an active hydrophobic form of factor H that is able to induce secretion of interleukin 1-beta or by human monocytes. *Eur J Immunol*. 1991;21(4):967–72.
35. Li T-R, Jia Y-J, Ma C, Qiu W-Y, Wang Q, Shao X-Q, et al. The role of the microRNA-146a/complement factor H/interleukin-1 β -mediated inflammatory loop circuit in the perpetuate inflammation of chronic temporal lobe epilepsy. *Dis Model Mech*. 2018;11(3):dmm031708.

Publisher's Note

Springer Nature remains neutral with regard to jurisdictional claims in published maps and institutional affiliations.

Ready to submit your research? Choose BMC and benefit from:

- fast, convenient online submission
- thorough peer review by experienced researchers in your field
- rapid publication on acceptance
- support for research data, including large and complex data types
- gold Open Access which fosters wider collaboration and increased citations
- maximum visibility for your research: over 100M website views per year

At BMC, research is always in progress.

Learn more biomedcentral.com/submissions

